UNIVERSITY^OF BIRMINGHAM

Sensitivity analysis and dynamic modelling of the reinjection process in a binary cycle geothermal power plant of Larderello area

Niknam, Pouriya H.; Talluri, Lorenzo; Fiaschi, Daniele; Manfrida, Giampaolo

[Link to publication on Research at Birmingham portal](#)
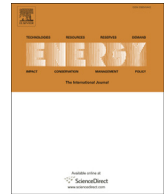
Sensitivity analysis and dynamic modelling of the reinjection process in a binary cycle geothermal power plant of Larderello area

Pouriya H. Niknam , Lorenzo Talluri , Daniele Fiaschi *, Giampaolo Manfrida

Dipartimento di Ingegneria Industriale, Università degli Studi di Firenze, Viale Morgagni 40, 50135, Firenze, Italy

ABSTRACT

The surface equipment design for a binary cycle geothermal power plant including facilities required for the power cycle and the complete reinjection process of two-phase geothermal fluid (H_2O + non-condensable gases (NCGs)) in the Castelnuovo area of Larderello are modelled. The proposed scheme includes the configuration of closed-loop power plant, NCGs compression train and reinjection process at the wellhead. Steady-state and dynamic simulations are performed. The steady-state model is developed to find the correct operating solutions and conditions, while the dynamic model investigates the unsteady behaviour of the system. The study includes a sensitivity analysis of surface equipment design, demonstrating the effect of internal and external variables on the system performance, including power cycle, compression train and reinjection process. The maximum compressor power consumption (at 60 bar reinjection pressure) is 176 kW at 8% CO_2 mass fraction into the geothermal fluid. The unsteady system behaviour at startup and its response to step-changes of flow stream condition is assessed: it is found that the average response-time is about 20 min. Also, the system requires a drain pressure higher than the saturation level for effective reinjection. A new Antoine − based correlation for water-CO_2 mixture is proposed for geothermal applications.

© 2020 The Authors. Published by Elsevier Ltd. This is an open access article under the CC BY license (http://creativecommons.org/licenses/by/4.0/).

1. Introduction

Geothermal energy is a sustainable and renewable energy alternative to the utilization of fossil fuels. Geothermal energy, even considering the high investment costs connected to well drilling, is still one of the viable solutions in several countries, boosted by the advancement in technology solutions. The benefits of increased deployment of geothermal energy include the feasible operability of over 7000 h per year and a high reliability, which is a critical issue for power grids. The geothermal power plants could achieve a very long lifetime if the geothermal field is correctly managed. The most crucial factor for a sustainable geothermal power plant is to guarantee the correct management of the reservoir, particularly of the reservoir water balance. This topic has been very delicate for decades, but thanks to the extensive utilization of condensate reinjection, it has been significantly tackled. Another relevant issue which is becoming the critical factor for a geothermal power plant in the last years is the release to the environment of non-condensable gases (NCGs), which are commonly found in natural reservoirs and can contain several types of contaminants (such as H_2S, NH_3 and heavy metals). Furthermore, even if the power plants CO_2 production is far lower than fossil fuel power plants [1], the average emission per geothermal plant is of about 400 g CO_2/kWh (with possible much larger values depending on the specific sites and the conversion technology [1]). Indeed, the CO_2 is found within the NCGs at high concentrations (exceeding 90% like in Italy) and is typically released at the cooling tower.

Treatment of NCGs is becoming a vital topic in the research and industry world, as environmental issues are predominating. The reinjection of geothermal fluids (after elimination of the NCGs) into the reservoir is a proven design in geothermal power plants but the reinjection of NCGs is a novel technology, which is still under development intending to decrease the environmental impact, tackling the emissions of CO_2 and H_2S. Several studies [2,3] confirm that only complete reinjection of NCGs provides a positive answer in terms of definite improvement of the sustainability issue. Some breakthroughs have been achieved in Iceland geothermal plants [4].

Several studies involve the modelling of geothermal power plants. These models are divided into two main topics: power

* Corresponding author.
E-mail address: daniele.fiaschi@unifi.it (D. Fiaschi).

generation and reinjection facilities (or alternative solutions for NCGs). The former includes the production well and the closed power cycle and the latter deals with the compressor train and the reinjection well.

The most suitable technology to be coupled to a "closed cycle reservoir" is the ORC technology. ORCs are promising systems for the conversion of a low-temperature geothermal heat source to power. Recently, several optimization and performance studies have been conducted to investigate the optimal configuration of ORC geothermal powerplants [5−7], as well as on the assessment of optimal working fluids [8,9], with particular reference to zeotropic mixtures [10].

Fiaschi et al. (2019) developed a power plant cycle simulation including organic Rankine cycle (ORC), compressor train, and the reinjection well emphasizing the exergy and exergo-economic analyses [11]. Recently, a hybrid geothermal-solar-biomass configuration was proposed by Moya et al. (2018), who developed on the concept of multipurpose energy generation [12]. Not only research has been conducted on power plant layout and optimization, but also on the reinjection process and facilities. Sohel et al. (2011) investigated the thermodynamic properties of the reinjection fluid including discharge temperature [13]. Lei et al. (2013) performed a simulation of the reinjection, with a particular focus on the reservoir obtaining the pressure profile of the reservoirs and calculating the permeability of various rock types [14]. Callos et al. (2015) simulated the two-phase reservoir to find the effect of CO_2-water reinjection process on the production well during the years by using the model of the Wairakei-Tauhara system [15,16]. Kaya et al. (2017) performed a sectional 1D and a 3D model by TOUGH2 simulator for the reinjection of NCGs-water mixture into the geothermal reservoirs investigating the energy recovery, and permanent trapping for several boundary conditions. The positive effects of the CO_2 reinjection on the production of the steam were also highlighted [17]. Shafaei et al. (2012) developed a 1D model including both the pipe and the annulus part of the reinjection well in which both water and CO_2 were injected into the saline aquifer. The model had a network configuration including sink, source, link, and junction nodes [18]. A geothermal power plant modelling including the compressor train, gas purification system, and reinjection unit was also developed by Manente et al. (2019) through the utilization of Aspen Plus to demonstrate an alternative solution of H_2S abatement to the current technologies (e.g. AMIS) [19]. Also, there are several other innovative separation technologies for the purification of the gas mixture commonly used in geothermal power plants and the natural gas industries [20,21].

Several studies represent configurations and arrangements of the power plant facilities and others investigate various aspects and parameters including the geothermal fluid thermodynamics or the geological investigation of the reservoir. Two significant topics of the system, which are the boundary condition effects on the power plant efficiency and the dynamic behaviour of the fluid through the reinjection well, are not much dealt by the literature, as they are emerging issues, which did not occur until new solutions, such as total reinjection, were taken into account. The first and second part of the current study are developed to try to fill these gaps. In the first part, a complete steady-state simulation is presented with specific detail of the equipment. The effect of the NCG content and reinjection pressure on the net power plant capacity is discussed by a comprehensive sensitivity analysis of the geothermal power plant including the power cycle and compressor train. The analysis is performed on a design based on the binary cycle concept in which an ORC is used instead of the direct exploitation of the geothermal fluid as the cycle working fluid. This configuration is a well-proven solution for power generation, which allows a separation of the heat source and the working fluid. The organic fluid selection

considerably affects the heat exchanger efficiency [22]. Two fluids of R245fa and R1233zd(E) are appropriate to be used as the working fluid because they are non-corrosive, non-flammable at the normal temperature and pressure [23]. In the present study R1233zd(E) was selected as it has a lower environmental impact than R245fa. The second part of the study deals with the dynamic behaviour of the drain injection in reinjection well, which is the link between the compressor train and the reservoir. The literature in this area suffers from lack of data; therefore, the objective of the dynamic simulation in the present study is to determine the unsteady behaviour of the re-injection process and, more specifically, the water within the inner tube. The results are promising for the wellhead sizing, drain valve selection, and the evaluation of both plant start-up and shutdown procedures. Besides, it can be taken into account in the analysis of risk for safety consideration.

To sum up, the main objectives of this research are (i) to provide an extensive analysis on a wide variety of boundary conditions of a novel power plant configuration, (ii) to assess the relationship between reinjection pressure and reservoir pressure and (iii) to estimate the flow pressure variations within the reinjection well.

In order to correctly achieve the above-mentioned objective, a case study has been selected. The selected geothermal power plant is designed to exploit the geothermal resource of the Montecastelli Pisano area, located in the eastern part of Anqua-Pomarance, within the vapour dominant field of Larderello.

2. Methodology

The present research consists of two different parts of the sensitivity analysis for the power cycle and the simulation of the reinjection well in which the detail is listed in Table 1.

The resource condition is expected to be saturated vapour at pressure of 60 bar and temperature of 280 °C at about 3500 m depth. Also, the pressure and the temperature at the production wellhead are estimated as 10.3 bars and 180 °C, respectively. The NCG mass content is estimated at 8% (7.8% CO_2 and 0.2% H_2S). The configuration consists of two production and one reinjection wells [27].

2.1. Model of the ORC

The scheme of the Castelnuovo power plant is shown in Fig. 1, displaying the power cycle, two production wells, and one reinjection well. A subcritical recuperative ORC power cycle utilizing *R1233zd(E)* as working fluid is fed (stream #3) through a condensing heat exchanger (MHE), which is pressurized at about 10 bars. The ORC scheme comprehends a pump (P), a turbine (T), a condenser (CON), an evaporator and a recuperative heat exchanger (RHE). The releasing of NCGs takes place at the top of the MHE (stream #40), while the condensed brine is released from the bottom of the MHE (stream #31) and directed to the reinjection well.

A three-stage intercooler configuration is considered for the compressor train design. The two intercoolers, a well as the precooler are of fundamental importance for the reduction of the compressor power. The removal of the condensate containing corrosive components (CO_2 and H_2S) from the bottom of the precooler (PreC) and the first intercooler (IC1) apart from improving compressor efficiency, also prevent the compressor failure due to the corrosion problems.

The steady-state model of the whole power plant is developed in EES software, exploiting the thermodynamic properties package and database. The power plant calculations are based on steady-state mass and energy balances (Eqs. (1) and (2)). The organic working fluid properties are taken from EES, while specific models
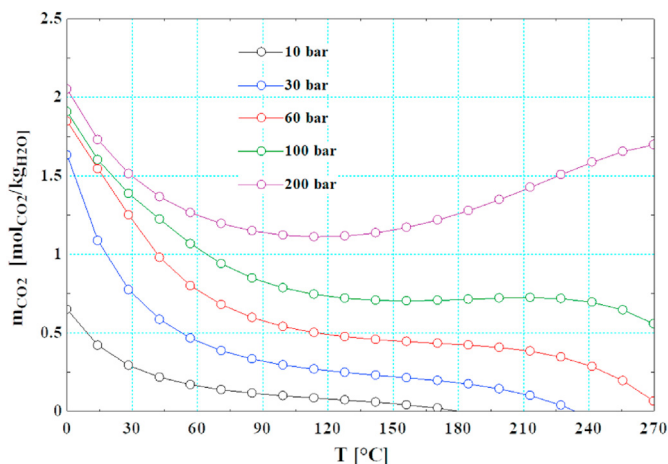
Table 1

Otuline of the simulations in the present research.

Part	Objective	Scope of simulation	Software	Approach
2.1	Sensitivity analysis	Surface facilities (the power cycle)	EES [24]	steady-state result screening for multiple cases
2.2	Two-phase fluid behaviour analysis	Reinjection well	UniSim [25,26]	Dynamic-mode (both steady-state and transient)

Fig. 1. Schematic of Castelnuovo power plants and wells/NCGs reinjection arrangement.

are developed for accurately calculate the geo-fluid properties (a mixture of H_2O-CO_2), using lookup tables to connect the data to the ORC simulation code. The turbine, pump, and compressor stages are assumed to be adiabatic devices. Negligible pressure losses occur in the components of the ORC and its piping system. Neglecting the changes of kinetic and potential energies, the mass and energy balance equations in the steady-state condition can be applied to each component.

$$\sum \dot{m}_i = \sum \dot{m}_e \tag{1}$$

$$\sum \dot{Q} + \sum \dot{m}_i h_i = \sum \dot{W} + \sum \dot{m}_e h_e \tag{2}$$

$\dot{Q}$ and $\dot{W}$ represent the heat and work transferred across the component boundaries, while $\dot{m}$ [kg/s] and h [kJ/kg] are the mass flow rate and the specific enthalpy of the streams.

The net produced power by the ORC can be expressed as:

$$W_{net} = W_t - W_p - W_c \tag{3}$$

The resource mass flow rate is estimated by the energy balance between the geothermal brine and the working fluid:

$$\dot{m}_{brine} = \dot{m}_{ORC} \frac{h_6 - h_3}{h_{30} - h_{31}} \tag{4}$$

The mass flow rate of the ORC is obtained by fixing the net power output of the turbine at 5 MW$_e$. The conditions are in line with the Italian laws; Legislative Decree no. 22/2010, amended by Legislative Decree no. 28/2011 and by article 28 of the Law Decree

of 18 October 2012, n. 179 has provided that in order to promote research and development of new geothermal power plants with reduced environmental impact, geothermal fluids with medium and high enthalpy are considered to be of national interest for testing pilot plants with reinjection of geothermal fluid in the same formations of origin and with nominal installed power not exceeding 5 MW$_e$ for each power plant [28]. The input data are summarized in Table 2. More details on the design may be found on Fiaschi et al. (2019) [11]; in the following sections, the sensitivity analysis to variable working conditions and the dynamic model results are discussed.

The model of Duan and Sun (2003) [29] - which is among the most reliable ones for CO_2 solubility in brines at high pressures and temperature - is replicated to be exploited in the current research. Fig. 2 shows the CO_2 solubility prediction for a wide range of pressure and temperature. In general, the molality of CO_2 gets higher with increasing pressure. On the other hand, the behaviour of molality vs. temperature varies depending on the operating pressure. Specifically, at high pressure, the molality of CO_2 has a

Table 2

Assumed design input data for the Castelnuovo power plant.

Parameter	Unit	Symbol	Value
Reference temperature	°C	T_0	15
Turbine isentropic efficiency	%	η_t	88
Pump isentropic efficiency	%	η_p	85
Geothermal fluid inlet temperature	°C	T_{30}	180
Geothermal fluid inlet pressure	kPa	P_{30}	1000
Net Power Output	kW	W_{net}	5000

Fig. 2. Reworked Model of Duan Z. and Sun R. (2003) for Water + CO$_2$ (no salts considered) Equilibrium calculations.

minimum, which is not present at low pressures. The equations of the model are reported in Annex A.

Most optimization studies for geothermal power plants are performed assuming that the geothermal fluid is pure water. In the present case, the resource (Castelnuovo Val di Cecina site, Italy) is in saturated steam conditions at a moderate pressure of 10 bar with an expected total NCGs mass content of about 8%; therefore the influence of CO$_2$ on the thermodynamic properties could not be neglected. In the process of heat transfer to the organic fluid, the geothermal fluid is condensed and most of the NCGs, which are mainly composed of CO$_2$, must be compressed and re-injected at a suitable depth in the reinjection well.

Considering the critical pressures of the fluids, it is assumed sufficient to define the CO$_2$−H$_2$O mixture properties with a third-order EOS model. This choice also derives from the fact that the thermodynamic model solves the system with high efficiency and reliability, with very reduced calculation time.

2.2. Dynamic model of the drain reinjection

The reinjection well is made up of a central pipe and a casing (Fig. 3). Along with the inner pipe, several points of injection (using specific reinjection valves) are installed to connect the annular space and the pipe. Water is injected into the pipe, while gas in the annular section will flow inside the main water flow through gas lift valves [30] placed at a depth depending on the practical water column, and it will finally form a mixed stream. Depending on the reservoir injectivity and the initial reservoir pressure that may be largely lower than the hydrostatic pressure for geothermal steam reservoirs, such as in Tuscany, Italy, the water column may not reach the wellhead, when water is injected at a constant flow rate. In this case, a "free fall" section is present at the top of the inner pipe. To allow gas injection in the water phase, at least one injection gas lift valve has to be located below the water level. The use of multiple injection points provides flexibility to operate in different situations, to facilitate the start-up operations and to secure the gas entrainment with the gas-liquid downward flow.

The reinjection of non-condensable gas and the condensed stream is a key part of the Castelnuovo geothermal power plant process. The drain stream coming from the condenser is re-injected through the inner pipe of the well. The inner pipe is filled with water, and the reservoir pressure naturally maintains the level of the water column. The re-injection process highly depends on how the re-injection pressure achieves equilibrium with the water level

in the well and is thus able to push the fluid mixture down into the reservoir successfully.

A specific simulation is arranged to determine the dynamic behaviour of the fluid from the drain valve to the mixing valve (MV). It is conducted to determine how the fluids proceed going down through the reinjection well (RW) under all the possible operating conditions and verify the size of the components. The dynamic simulation can also be used to either estimate the time required for achieving steady-state conditions after any step changes in drain pressure or drain flow rate. This data is used in the control system, which is expected to maintain the water level within a specific acceptable range inside the Main Heat Exchanger (e.g. condenser MHE). The simulation also addresses the essential control characteristics of the actuator valve.

Fig. 3 shows a schematic of the reinjection well. The current model considers only the drain valve and the internal pipeline of the drain stream, as these are the main components influencing the reinjection process.

The outer (gas stream) pipe is not considered in the current simulation, as it has no direct effect on the hydrodynamics of the drain injection. The only accounted perturbation from the annular section is the one due to the heat transfer, which occurs between the inner liquid and the outer CO$_2$, concurrently flowing in the annulus. The heat transfer mechanisms combine convection and the conduction, which take place between the fluid flowing within the inner tube and the fluid in the annulus section. The reference temperature outside the annulus wall is considered as a fixed value of 89 °C. (as shown in Table 3), as the CO$_2$ temperature undergoes only a minor increase because of the geothermal underground temperature gradient.

The Honeywell's UniSim® Design Suite [25,26] is used to simulate the reinjection well from wellhead to the reservoir both in steady-state and dynamically. The calculations take into account the temperatures, pressures, and volumes of the mixture going down through the well, starting from the wellhead equipment. The well is simulated in the form of a vertical pipe in UniSim. The length, elevation, and the type of pipes match with the geometry of the well. There are several factors to consider in the well design, and the most significant one is the flow model, which is responsible for the pressure drop and the friction within the pipe. In the present model, the Beggs & Brill correlation [31] is selected. It is applicable over a wide range of pipe sizes and flows directions, and particularly for downward vertical flows. All the thermodynamic properties including the compressibility, solubility and the density of all components of the mixture along the pipe are calculated based on sour-Peng Robinson Equation of State (sour-PR EoS) available in the UniSim® package [25,26]. This EoS is suitable for simulating two-phase geothermal fluid equilibrium in a wide range of pressures and temperatures. Niknam et al. used this EoS as the reference approach for the prediction of CO$_2$ and H$_2$S solubility in water which matches with the reinjection process [32]. The application of this EoS is extended to the optimization and process simulation of the geothermal surface facilities in geothermal application e.g. the gas purification within the geothermal powerplants [33] The sour-PR result is compared with some other well-known models (PR, SRK, and sour-SRK) and PHREEQC [34], the latter being a specific software for geothermal calculations. The Comparison is performed at the feed condition of Castelnuovo case study and Fig. 4 demonstrates the results for the solubility of both H$_2$S and CO$_2$ in the water.

The supporting idea for using the sour-PR model is that it combines the PR equation of state and Wilson's API Sour method for achieving accurate solubility of CO$_2$ and H$_2$S in the water, in which the K-values for the aqueous phase are calculated using Wilson's method for considering the ionization of the H$_2$S and CO$_2$,
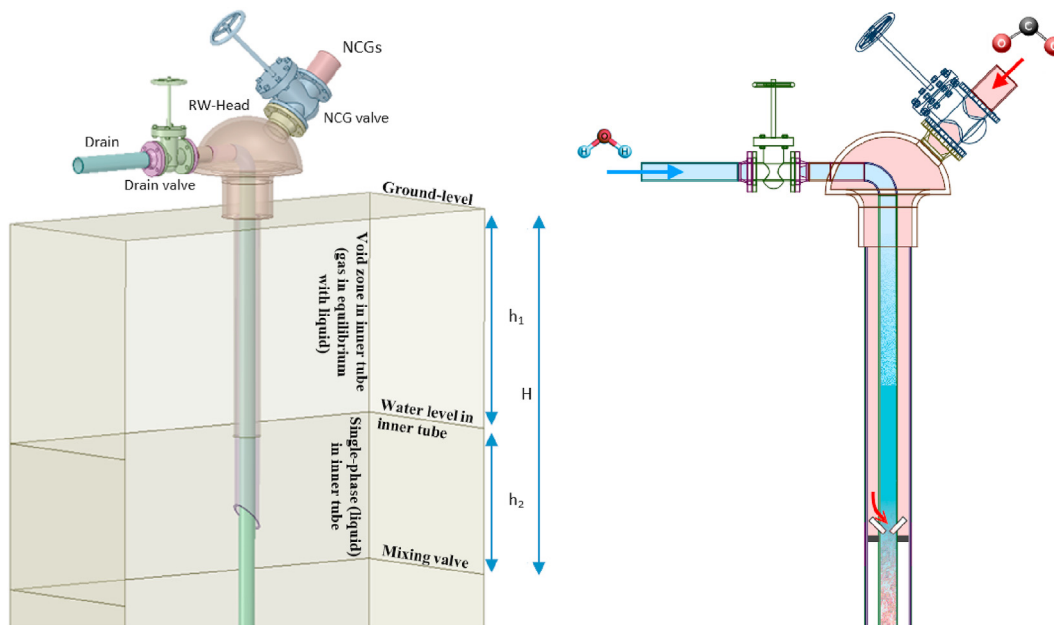
Fig. 3. NCG/drain reinjection well (RW) configuration.

Table 3
Boundary conditions and process equipment detail.

Equipment or Boundary conditions	Design TT	Design TP
Drain composition (wt %)	H_2O …. 99.52	
	CO_2 …. 0.44	
	H_2S …. 0.04	
Drain (inlet) Pressure (kPa)	1000	
Drain (inlet) Temperature (°C)	89	
Inlet fluid condition	subcooled	
P^{sat} at Drain Temperature (kPa)	882.7	
Equation of state	Sour PR	
Drain Valve size (inch)	3.5″, ($C_v = 500$)	
All Line size	3.5″	
Controller reading, set point	Drain mass flow, 16 kg/s	
Controller target	Drain valve opening (%)	
Valve action	Equal percentage	
Controller Type	PID	
Controller constant (K_c , $\tau_i(min)$, $\tau_d(min)$)	0.1, 0.2, 0	
Well part A (Type: Diameter - Height)	Tank: 0.09 m, 50 m	
Well part B (Type: Diameter - Height)	Tank: 90 mm 550 m	Pipe: 90 mm 550 m
Heat transfer principle	Convection from the Tank/Pipe wall, ($T_{ref} = 89$ °C)	
Pressure loss source	VLV-2	Pipe flow correlation
nozzle size (all inlets & outlets) (inch)	3.5″	
Vent valve opening (%)	0%	
Vent pressure (kPa)	100	
Interconnection valve opening (VLV-1)	100%	–
Valve specification (VLV-2)	$\Delta P \cong 74.4\ kPa/100m$	–
Drain Out Pressure (kPa)	6000	–
PI stream	Pressure Indication (Zero flow)	–

in the aqueous water phase. The aqueous model employs a modification of Van Krevelen's original model and overcomes the limitations. The K-value of water is calculated using an empirical equation, which is a function of temperature [35].

Prior to discussing the simulation software schematic, it is necessary to review the principle of reinjection process. The reinjection process works according to the principle of the pressure balance between the sum of all pressure components (P_{total}) and the pressure at the bottom of the well. The bottom points can be defined as either the reservoir pressure or the pressure of the point where the NCGs is mixed with water by the mixing valve (MV).

Therefore, according to Eq. (5), the total pressure should be at least equal to the pressure of the mixing valve (P_{MV}), which is one of the necessary input of the simulation.

$$P_{total} = P_{MV} \tag{5}$$

This governing equation is the preliminary constraint for achieving a steady-state injection. Referring to Eq. (6) and Fig. 3, the components of P_{total} are the overhead pressure of the trapped gas (P_1) which is constant over the total gas column height, h_1, the static head of the water level (P_2) corresponding to the water column h_2, decreased of the pressure drop caused by friction between
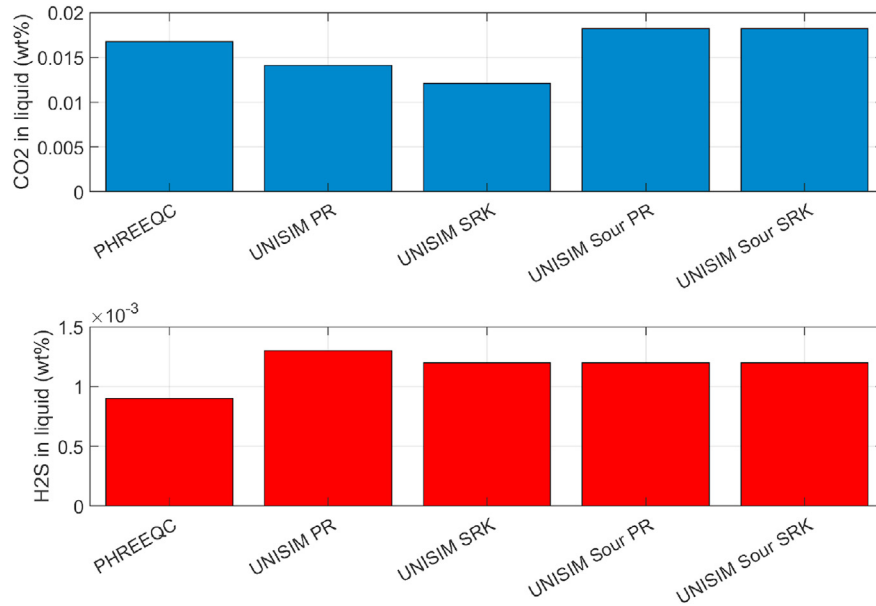
Fig. 4. Solubility of CO_2 and H_2S in Castelnuovo feed condition (Condition of 89 °C, 1 bar).

the fluid and the tube walls.

$$P_{total} = P_1 + P_2 - \Delta P \tag{6}$$

In the present simulations, for an accurate estimation of the water level, P_2 is divided into two contributions A and B, which are described in the next section.

$$P_{total} = P_1 + (P_{2A} + P_{2B}) - \Delta P \tag{7}$$

The schematic of UniSim simulation is shown in Fig. 5, including two approaches for the simulation of the drain injection process. The model includes the control of the flow rate by valve throttling and estimation of the water level. The drain valve and the controller are the same for both cases and are used to adjust the valve opening and determine the water level. In the first design (Tank-Tank: TT), the well is simplified with two cascade tanks and a valve, while a preliminary cylindrical tank and a pipe segment are utilized in the second one (Tank-Pipe: TP). The details of the equipment models are listed in Table 3.

The first simulation option (TT) gives the approximate level of
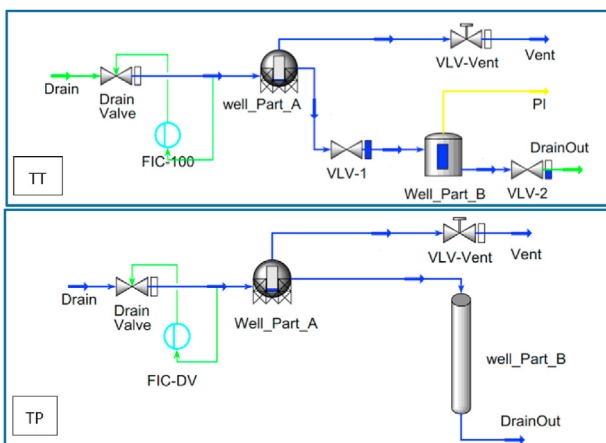
the water and the value of friction loss along the well depth; in the next step, the alternative approach of (TP) is activated to provide the final simulation considering the pipe flow correlation (which takes into account friction losses).

The model has fixed pressure boundary conditions, both at the inlet and the outlet (MV). The continuous reinjection of the condensed steam is vital for safety concerns, maintaining the desired heat exchanger performance, and the circulation of the flow through the plant. A controller is considered defining the desired mass flow rate, which is expected to be the whole condensate stream formed inside the condenser. A fixed total downward 600 m length is considered as a negative vertical elevation, which contributes to the maximum pressure of 60 bar (non-flowing water column head).

The pipe section is divided into 200 segments to allow sufficient accuracy; the applied model is capable of evaluating possible multiphase conditions. However, in the final simulation design (TP) the tank height (part A) and the length of the pipe (part B) are considered so that the water level remains within the tank (part A). Consequently, the flow remains in single liquid phase conditions through the whole pipe segment. In the dynamic simulation, the water level of the well is the criteria for determining the state of the simulation and the solutions are considered as steady once the water level becomes stable for more than 5 min. The dynamic simulation provides data on the reinjection and performance of the equipment from the surface level to the depth of the well. The unsteady model is focused on the managing of two-phase flow concerning the water level estimation, mass flow adjustment, friction loss estimation, and calculating the time needed to reach the final steady condition. Knowledge of the process constraints helps to guarantee the full reinjection of the drain under the two-phase condition.

3. Results

3.1. Sensitivity analysis of power cycle

The first parameter considered in the sensitivity analysis of the Castelnuovo power plant is the CO_2 content in the geothermal

Fig. 5. PFD of the dynamic modelling of the injection process Design TT and Design TP.

resource. As expected, lower CO_2 content corresponds to lower required compressor power and thus higher cycle thermodynamic efficiency. However, due to a better match between the main heat exchanger curves, the exergy efficiency increases with increasing CO_2 content into the geothermal fluid stream: it suggests better exploitation of the resource. The key results of the performance calculations are collected in Table 4.

Also, Table 5 resumes the effect of CO_2 content at a fixed design power output of the power plant (5 MW_e), while Fig. 6 shows the combined effects of the power plant and CO_2 content on the required NCG recompression work. Specifically, the maximum expected compressor power consumption (for 60 bar reinjection pressure) is 176 kW at 8% mass fraction content of CO_2 into the geothermal stream, referring to an 8 MW_e power plant size (corresponding to the maximum expected flow rate of the production wells, that is 18 kg/s).

The boundary conditions of the systems are also analysed, such as power output (which directly influences the extracted mass flow rate of the geothermal fluid) and the reinjection pressure of the NCGs. Fig. 7 resumes the variation of compressor work at variable power output and reinjection pressure conditions.

In order to understand the influence of the compressor efficiency, a sensitivity analysis is carried out varying the compressor efficiency in a reasonable range (65–89%), at different possible nominal values of power output. Fig. 8 shows the contour plot of Compressor power demand as a function of compressor efficiency and net plant power output.

Finally, the heat duty of each inter/after-cooler of the compressor train is analysed. Notably, the scheme is composed of one Pre-cooler, two intercoolers, and one post cooler. The maximum heat recovered from the heat exchangers at the highest possible $\%CO_2$ and P_{reinj} is 24 kW, 61 kW, 70 kW, 143 kW for PC, IC1, IC2, and PostC, respectively. Fig. 9 shows the Heat duty of each heat exchanger at variable $\%CO_2$ and P_{reinj}.

3.2. Response time of the reinjection well

By the present simulation, an investigation is carried out to give an estimation of the approximate time required to reach the steady-state condition during the reinjection system start-up. Referring to Fig. 5, the initial value of the simulation considers the well part A to be totally or partially filled with the nitrogen at atmospheric pressure and temperature. In the next step, the simulation is performed with real injection condition to evaluate the necessary time to reach the steady-state condition. The initial condition for the simulation is selected as the natural water level according to the static head of the non-flowing water; the remaining volume or the wellhead is filled with nitrogen at atmospheric pressure and temperature at 25 °C. Starting from zero time, the valve opening changes from zero to the desired percentage corresponding to the expected flow rate. Principally, the water level starts to rise or fall once the mass flow rate changes by adjusting the control valve. The operational sequence for the start-up of the reinjection starts with opening the drain valve; therefore, the mass flow increases, the drain pressure takes part in the

pressure balance and, consequently, the water level drops. As shown in Fig. 10, the dynamic simulation gives the time-dependent profile of the water level, where the approximate time for different cases is almost invariable and is found to be less than 20 min approaching to a stable condition of water level.

Another significant aspect is dealing with the consequences of adjusting the mass flow rate, either manually or automatically, within the capacity of the piping design. The settling time for a step response of the system can be found as the result of changing the inlet mass flow rate. The design value of the drain mass flow rate for Castelnuovo geothermal plant is about 16 kg/s and four alternative cases including one +10% increasing step and three −10% decreasing steps in mass flow rate are assessed. The step response of water level is shown in Fig. 11 for three decreasing steps of mass flow rate, which are applied through the control of the valve opening percentage. Also, in this case, the required time for adapting the water level to new inputs is about 20 min.

3.3. Pressure losses and valve operation

By exploiting the results of the previous simulation, the role of the drain valve is determined. The uniform percentage principle is considered for the valve opening and both the valve opening and the water level profiles corresponding to different mass flow rates are shown in Fig. 12a. Also, the corresponding valve ΔP_{valve} and $\Delta P_{friction}$ are calculated, and are shown in Fig. 12b. Both pressure drops are negligible compared to the feed pressure, but the magnitude and the direction of their changes are different and interesting to analyse. ΔP_{valve} changes with an average slope of $+0.25\ kPa/+1\%\ \dot{m}$ while $\Delta P_{friction}$ changes with an average slope of $-6.25\ kPa/+1\%\ \dot{m}$. More flow contributes to increased friction losses, thus, the system increases the height of the water column to counterbalance this pressure loss. Another result from the valve opening process-as shown in Fig. 12a-is that the selected valve size is correct because with the desired flow rate only 35% of the valve or line flow capacity is used.

3.4. Flow-pressure variations in the reinjection well

In order to define the right boundary conditions of the reinjection system, it is essential to assess the behaviour of the equipment under different reinjection pressures and other operating conditions. The simulation is carried out for different gas delivery pressures to the reinjection well, including the maximum foreseen pressure of 60 bar as the reference condition. The previous configuration in Fig. 5 (TP) is rearranged as a multi-stage array of tanks (MTP) for the preliminary section to allow the analysis of the water level over a wider range.

In this part of the study, the role of P_{MV}, P_1 and the feed condition is analysed. In order to have a better understanding of the magnitude of different pressure components, the analysed process is schematized as follows. The pressure components (according to Eq. (6)) for the case of $P_{MV} = 60\ bar$ is

$$P_{total} = (P_1 = 9\ \text{bar}) + (P_2 = 55.4\ \text{bar}) - (\Delta P = 4.4\ \text{bar}) \tag{8}$$

Where P_2 corresponds to the pressure of 590 m of water column ($\rho_{water\ @\ 9bar,\ 89°C} = 958.\ \mathbf{kg/m^3}\ g = 9.8\ \mathbf{m/s^2}$) and ΔP is the friction loss, which is calculated with the average ratio of 0.744 bar/100 m P_2 has a dominant role in satisfying Eq. (7) constraint and approaching the steady-state condition. Therefore, for the analysis of P_2 it is necessary to rearrange the simulation model to the form of Fig. 13 in order to be able to achieve the water level in a wide

Table 4
Main calculated performance parameters for the Castelnuovo Power Plant.

Parameter	Unit	Symbol	Value
Geothermal mass flow rate	kg/s	$\dot{m}_{geo}$	11.82
CO_2 mass flow rate	kg/s	$\dot{m}_{CO_2}$	0.9452
Power plant efficiency	%	η	18.56
Heat input from Geothermal Fluid	kW	$\dot{Q}_{HE}$	26855

Table 5
Performance and working parameters behaviour for a 5 MWe power plant at variable CO_2 content in the geofluid (reinjection pressure and compressor efficiency of each stage are fixed at 60 bar and 0.82 respectively).

Cases		$\dot{W}_{net}$	W_{c1}	W_{c2}	W_{c3}	W_{ctotal}	$\dot{m}_{30}$	$\dot{m}_{31}$	$\dot{m}_{40}$	$\dot{Q}_{HE, GEO}$	η_I	η_{II}
		[kW]	[kW]	[kW]	[kW]	[kW]	[kg/s]	[kg/s]	[kg/s]	[kW]	–	–
%CO2 Variation, W_{net} = 5 MW, P_reinj = 60 bar, eta_c = 0.82	0.5%CO_2	5000	2.537	2.459	2.311	7.307	10.77	10.71	0.05384	26221	0.1906	0.5443
	1%CO_2	5000	5.105	4.947	4.65	14.7	10.83	10.72	0.1083	26260	0.1903	0.5462
	2%CO_2	5000	10.33	10.01	9.414	29.76	10.97	10.75	0.2193	26339	0.1897	0.5498
	4%CO_2	5000	21.19	20.53	19.3	61.02	11.24	10.79	0.4496	26503	0.1884	0.557
	6%CO_2	5000	32.6	31.59	29.7	93.89	11.53	10.84	0.6918	26675	0.187	0.5645
	8%CO_2	5000	44.62	43.24	40.65	128.5	11.84	10.89	0.947	26856	0.1856	0.5721
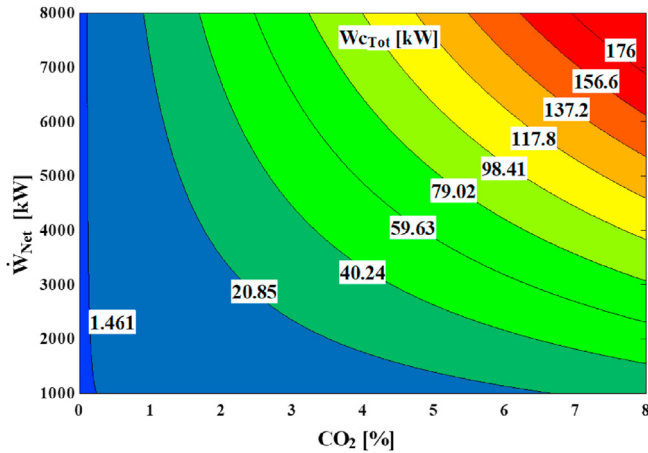
Fig. 6. Total required NCG recompression power at variable powerplant size and CO_2 content into the geofluid.
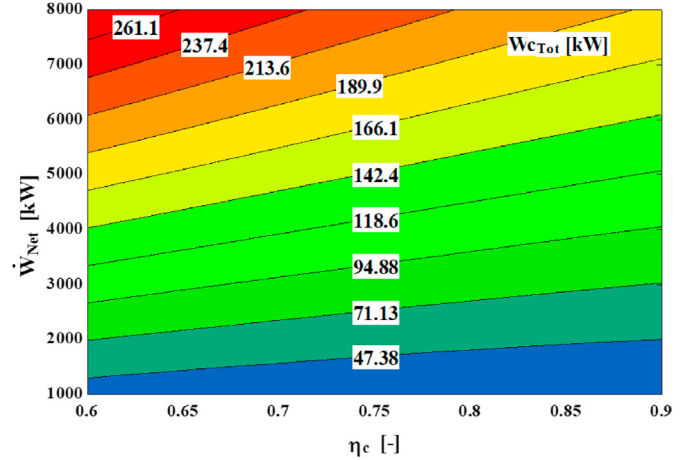

Fig. 8. Required NCG recompression power at variable η_c and $\dot{W}_{net}$.
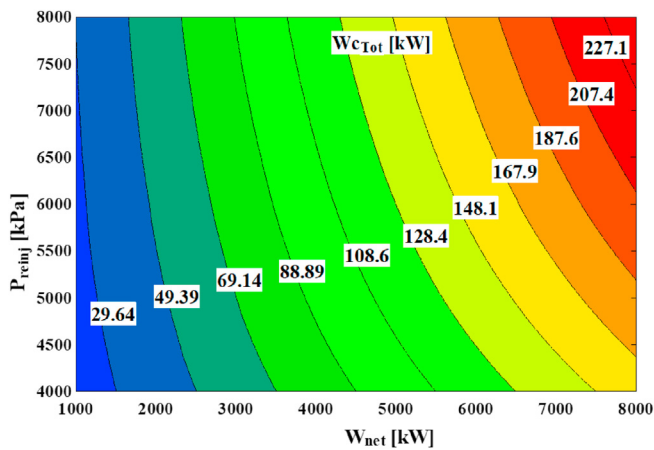

Fig. 7. Required NCG recompression power at variable brine reinjection pressure (P_{reinj}) and powerplant size ($\dot{W}_{net}$).

range of P_{MV}. In the new configuration, the maximum of the 200 m void level can be simulated using four 50-m-height cascaded tanks. The inputs of the model are both the top and the bottom pressures; then, a reasonable initial guess for the water level is necessary for the convergence of the calculations.

The corresponding equation of the new arrangement is described by Eq. (9):

$$P_{total} = P_1 + \left(\sum_i P_{2A,i} + P_{2B} \right) - \Delta P \tag{9}$$

The water level inside the well can be calculated by evaluating the conditions at which the static water column matches the prescribed pressure at the well-mixing valve (MV). Since the actual drain valve operating pressure and the value of the well-MV pressure necessary to realize the required injectivity in the reservoir are unknown at the preliminary stage, a sensitivity analysis is set up for these variables. The sensitivity analysis helps to understand the behaviour of the water level in the RW and the injection quality. Four different P_{MV} values of 45, 50, 55 and 60 bar are considered for each of them; the simulation is also conducted in different values of P_1 with the upper bound of 10 bar.

The results are illustrated in Fig. 14, showing the profiles of the free water level at different values of P_{MV} and P_1; in all cases, the lower pressure limit for re-injection (referring to a mixture with about 8% CO_2 content) is determined by the saturation conditions.

In all of these case studies, the drain composition is fixed. The related saturation pressure does not change, and it is represented in Fig. 14 as a vertical line. The behaviour of the reinjection system is significantly different when the feed is located in the subcooled or the two-phase zones. The common fact in both cases is that the system tends to stabilize the pressure at the wellhead (which is the same as the drain valve outlet pressure) at the value of the saturation condition or at least to minimize the gap between the operating thermodynamic state and the saturation condition.

The Subcooled feed is entirely under control by the drain valve opening, and steady conditions are achieved quickly. Also, the controller adapts the valve opening to preserve a fixed drain flow rate, and thereby, the water column level would not be changed in subcooled condition. With the subcooled feed, the drain valve outlet pressure and the wellhead pressure will be stabilized at the saturation value, which is lower than the primary feed pressure; ΔP_{valve} is adjusted by the controller.
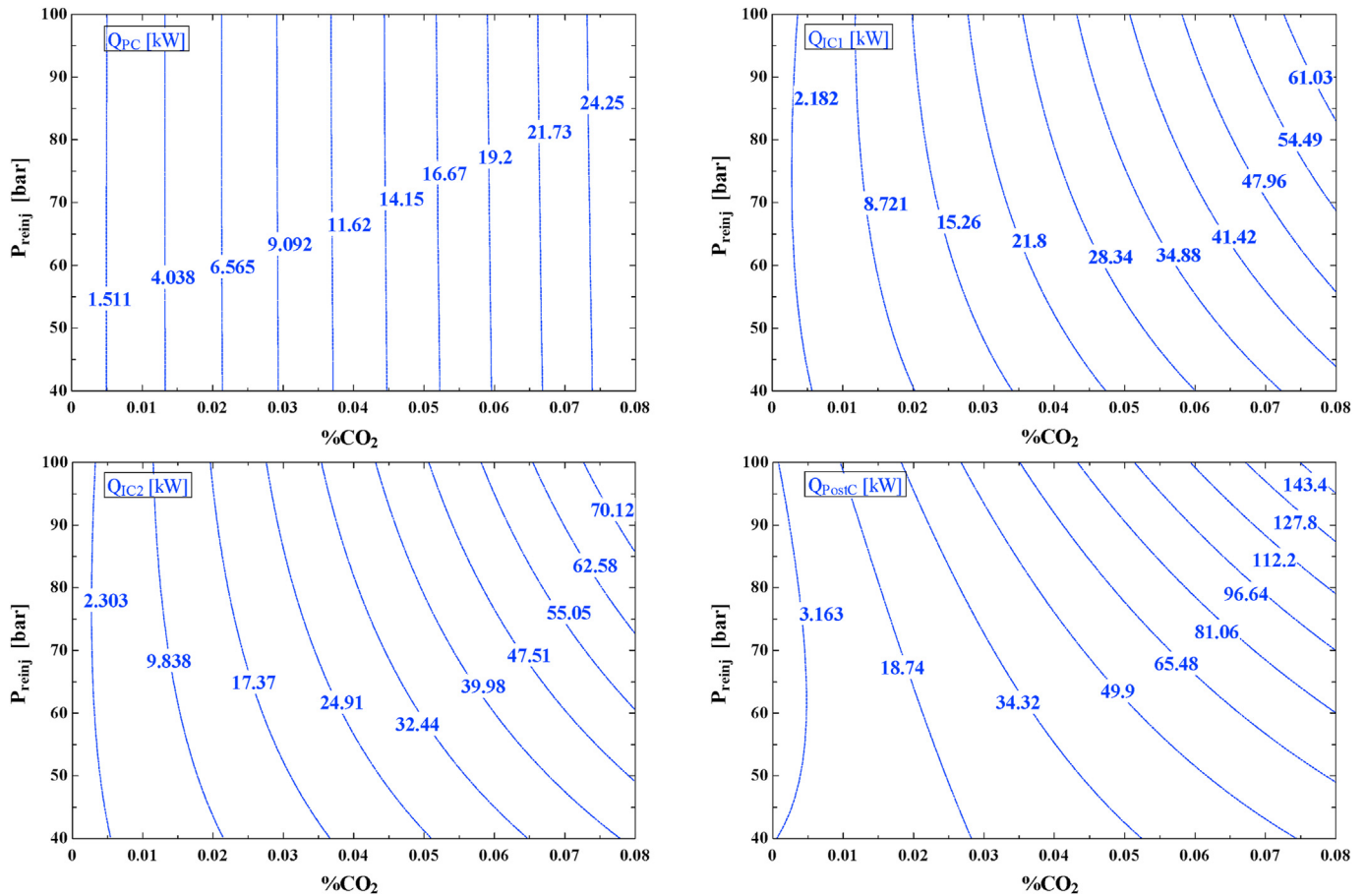
Fig. 9. Heat duty of the heat exchangers in the compressor train vs P_{reinj} and $\%CO_2$.
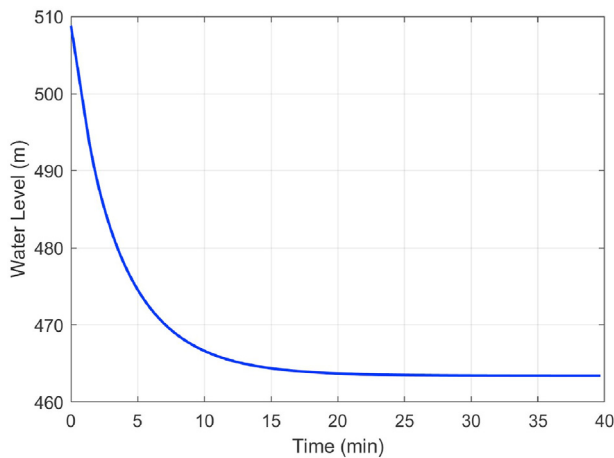

Fig. 10. Stabilization time of water level (base level: -600 m) in the start-up phase (Selected case study for the figure: $P_{in} = 10$, $P_{MV} = 50$).
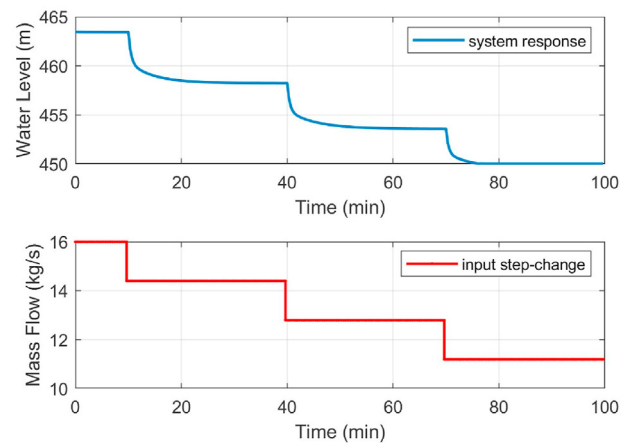

Fig. 11. Water level (base level: -600 m) change resulting from three reduction steps applied to the valve opening. (Reducing mass flow rate -10%, -20%, and -30%).

The two-phase feed, even with 1% of vapour, represents a challenge. Following the natural trend to saturation conditions, when the system is fed at a pressure lower than this value (the red zone in Fig. 14), the gas volume is continuously growing at the top section and the pressure is gradually increased. This increase has the upper limit of the feed pressure but there would be no limit for the gas volume. After a while, the gas pocket volume gradually increases, and pressure reaches the maximum possible value (Main

heat exchanger); this process contributes to determining a lower water level in the reinjection well. The liquid fraction - which is in saturation conditions - has no more capacity to accept additional dissolved gas moles. Also, the fresh feed continuously adds new vapour to the system. Thus, for $P_1 < P^{sat}$, the pressure at the drain valve outlet is driven to P^{sat}, and the valve opening approaches 100%; under these conditions, the controller becomes ineffective, the value of P_2 decreases and the system never comes to a stable
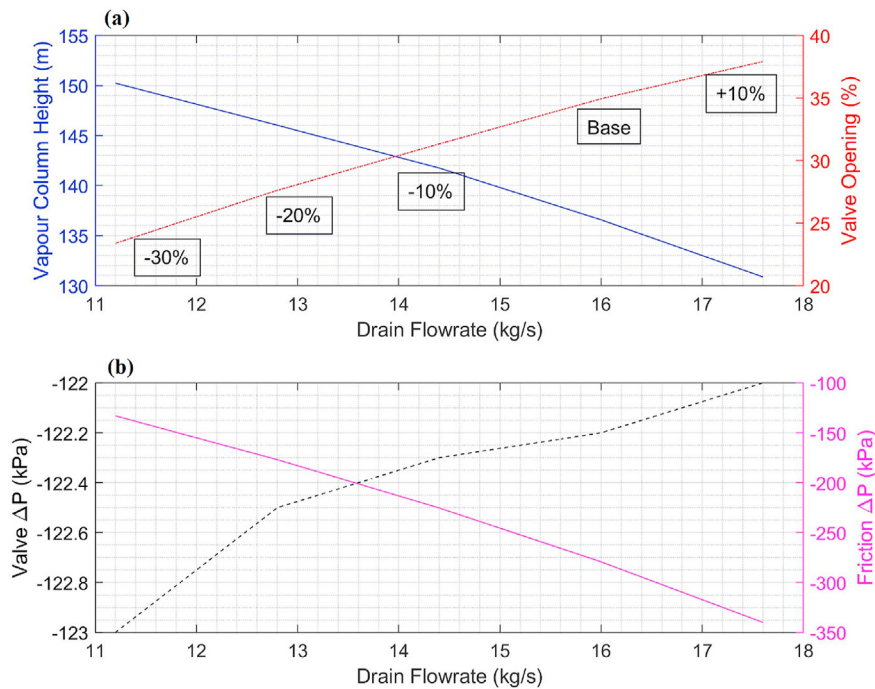
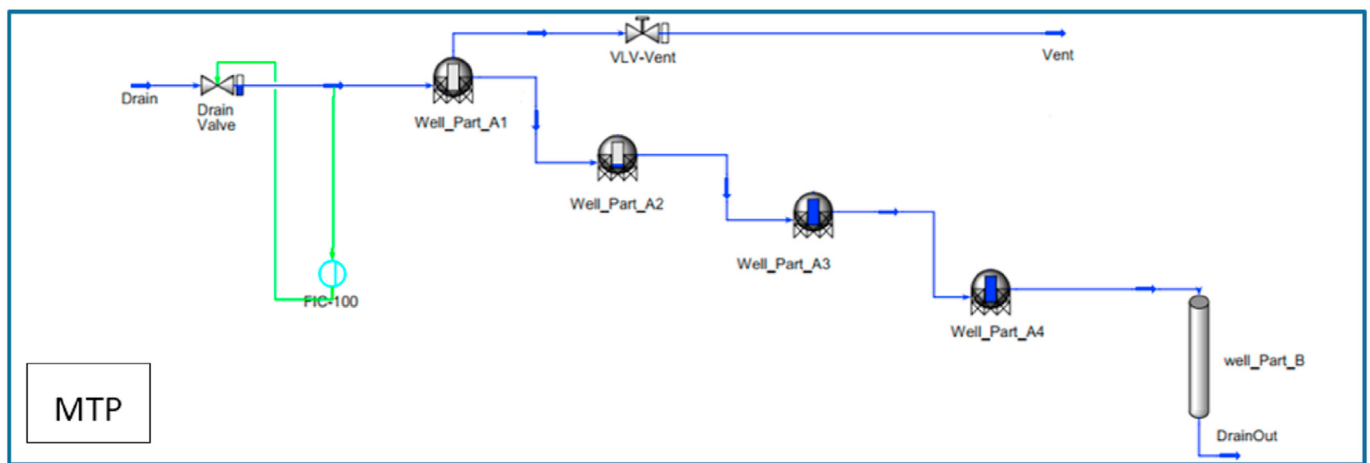**Fig. 12.** The relation of different process parameters to the mass flow rate.

Fig. 13. The model schematic for water level estimation in different well-MV pressure (Design multi-tank with pipe: MTP).

status. An important aspect, even more substantial than all the above-described effects, is that the mass flow rate gradually approaches zero with decreasing ΔP across the valve. The black arrows in the unsteady zone or zero-flow-approach area indicate that the water level is slowly decreasing.

As a result, the re-injection is kept under control only if the drain stream flows to the drain valve either with equal or higher pressure than the saturation condition (the yellow zone in Fig. 14) in which no initial gas volume is present before the drain valve. On the other hand, P^{sat} depends on the temperature, so temperature may be the variable, which can be considered to adjust P^{sat} in the right conditions. Table 6 shows the proposed saturation pressure correlation for water-CO_2 mixture. The formulation of the model is based on the Antoine equation [36] with additional coefficients related to the CO_2 content. The reference data for the correlation are the results of

the Sour-PR EoS in UniSim® software within the temperature range of $0-100\ °C$. The correlation coefficients are derived using the genetic algorithm in the form of minimization approach [32,37]. The saturation pressure calculated by the correlation is a minimum value for the drain stream, which keeps the fluid in sub-cooled condition and helps the system to attain the desired steady-state condition. It is also a substantial technical limit to provide an adequate safety margin for the reinjection well, while a lower drain pressure possibly causes the process failure.

The addressed problem can be solved with suitable interventions. These include guaranteeing a sufficient piezometric head between the main heat exchanger and the reinjection well, or by the provision of a circulation pump between the two components.
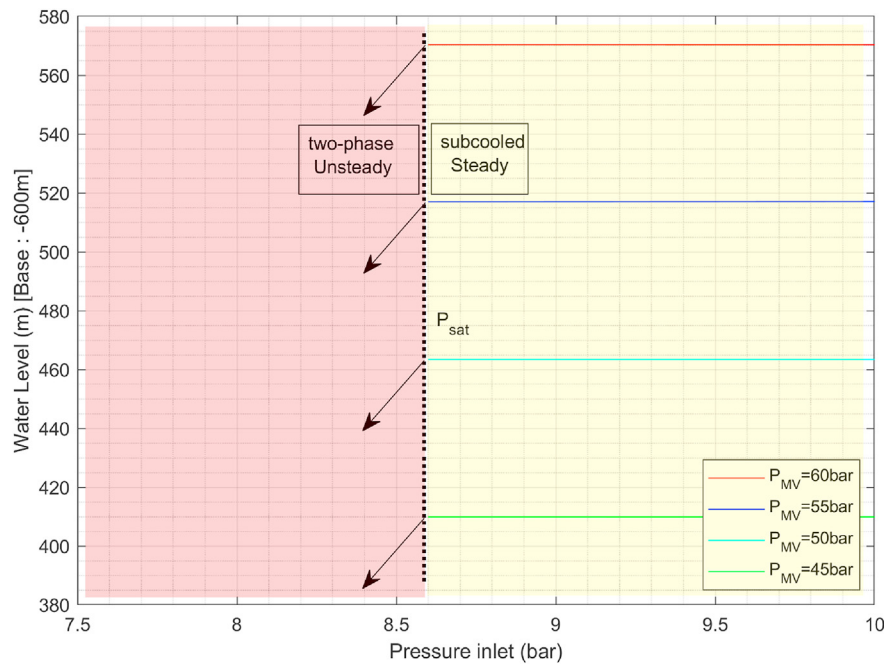
Fig. 14. Effect of feed pressure and feed condition on the water level ($P^{sat} \cong 8.6$ bar).

Table 6
The coefficients correlated for saturation pressure of water-CO_2 mixture.

fluid	Modified Antoine Equation $\log_{10}(p) = A - \dfrac{B_0 + B_1 x_{CO2}^{B2}}{[C_0 + C_1 x_{CO2}^{C2}] + T}$, $p[mmHg]$, x_{CO2} : weight fraction), T:$^\circ C$						
	A [36]	B_0 [36]	B_1	B_2	C_0 [36]	C_1	C_2
Pure water	8.07131	1730.63	0	0	233.426	0	0
Water + CO_2			957.8	0.03073		963.9	0.229

3.5. Solubility of NCGs in depth of the RW

As discussed in the previous sections, the mixing valve (the re-injection gas lift valves) represents the connection between the outer pipe (high-pressure NCGs) and the inner pipe of the RW (high-pressure liquid), which is going towards the reservoir. The solubility of NCGs in water increases with increasing pressure (depth). The liquid in the inner pipe is not pure water and it has some dissolved NCGs, due to the saturated drain reinjection at the RW head.

An analysis is performed using the same thermodynamic model described in the previous sections (Sour-PR, UniSim®) to assess both the occupied and free capacities of the liquid in the inner pipe at different pressures, which correspond to different possible reinjection valve depth. As shown in Fig. 15, the free capacity is a measure of the amount of NCGs coming from the outer pipe (through the MV) which can be dissolved. In this analysis, the temperature parameter is fixed at 89 °C, where the saturation pressure is into the 8–10 bar range (the exact value depends on the EoS and impurities). At about 10 bar, which is the minimum suggested design pressure of the drain reinjection at RW head, the capacity is almost entirely occupied by the already dissolved CO_2, thus, this fraction is reduced. On the other hand, the "free capacity" increases with nonlinear behaviour with increasing pressure, because the overall solubility of the NCGs in pure water is increased up to 85% at 60 bar. As a result, both applying higher pressure for the drain and placing the MV at a deeper level allow an increase of

the reinjection efficiency. Also, a marginal portion of CO_2 solubility capacity is occupied by the H_2S, which however, decreases with increasing pressure. Thus, the main concluding remark of this section is that, in a full reinjection scenario (water and NCGs), the CO_2 and H_2S content of the drain should not be neglected.

4. Conclusions

In this study, a full scheme of Castelnuovo power plant is presented with a focus on power generation performance and the reinjection process. The present discussion includes two parts of a detailed model of the surface equipment in steady-state condition and an unsteady simulation of the reinjection well. A sensitivity analysis is carried out and the performance of the system for the power generation and the compression train are assessed over a wide operating range. The sensitivity analysis confirmed the expected impact of CO_2 content on the power consumption of the reinjection compressor, achieving the maximum value at 60 bar reinjection pressure and 8% CO_2 content. A particular trait of this analysis is the exploitation of the heat released by the intercoolers, which, in case of a high content of CO_2, as well as a high required pressurization, can allow a significant heat production of about 300 kW. A dynamic model is developed for the reinjection process to examine the unsteady behaviour of the well from the surface to the reservoir. The results help to manage the two-phase flow condition at the inlet effectively. It is found that the content of CO_2 plays a crucial role in maintaining a steady-state condition. It is
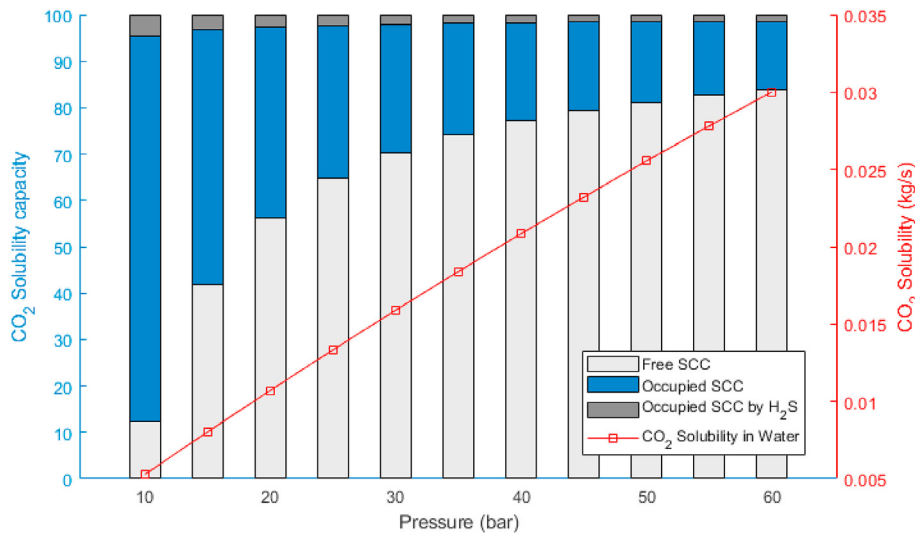
Fig. 15. Solubility Capacity of CO2 versus pressure (corresponding to depth)[Drain composition: Table 2, at Saturation condition].

discussed that the corresponding saturation pressure is a minimum threshold criterion for the liquid injection and, therefore, a correlation is derived for the saturation pressure of the mixture, which is applicable to a wide range of CO_2 fractions and temperatures. Moreover, an average of 20 min response time is found for the reinjection system, which is required for the design of the valve and the related controller. The CO_2 content in the drain has an important influence on the NCG injection in terms of the solubility. At the pressure of 10 bar most of the capacity is already occupied by the previously dissolved CO_2 and the share of the free capacity increases with a nonlinear behaviour of the pressure up to about 85% at 60 bar. The presented sensitivity analysis and the dynamic simulation represent a significant advancement to the current state of knowledge of the reinjection well behaviour, allowing the assessment of the most critical parameters of the process. It is of special relevance in geothermal fields characterized by relatively high amounts of NCGs mixtures like the Larderello area case study here discussed.

CRediT authorship contribution statement

Pouriya H. Niknam: Methodology, Software, Investigation, Validation, Writing - original draft. **Lorenzo Talluri:** Formal analysis, Methodology, Investigation, Resources. **Daniele Fiaschi:** Conceptualization, Writing - review & editing, Supervision, Funding acquisition. **Giampaolo Manfrida:** Conceptualization, Writing - review & editing, Project administration, Funding acquisition.

Declaration of competing interest

The authors declare that they have no known competing financial interests or personal relationships that could have appeared to influence the work reported in this paper.

Acknowlegment

List of symbols

EoS	Equation of State
h_3	Enthalpy of Main heat exchanger (MHE) inlet (ORC), [kJ/kg]
h_6	Enthalpy of Main heat exchanger (MHE) outlet (ORC), [kJ/kg]
h_{30}	Enthalpy of Main heat exchanger (MHE) main feed, [kJ/kg]
h_{31}	Enthalpy of Main heat exchanger (MHE) drain (condensation), [kJ/kg]
$\dot{m}_{30}$	Mass flow rate of Main heat exchanger (MHE) [kg/s]
$\dot{m}_{31}$	Mass flow rate of Main heat exchanger (MHE) drain (condensation) [kg/s]
$\dot{m}_{40}$	Mass flow rate of Compressor train [kg/s]
$\dot{m}_{WF}$	Mass flow rate of working fluid organic cycle [kg/s]
MHE	Main (condensing) heat exchanger
MTP	Multi-Tank-Pipe
MV	Mixing Valve
NCG	Non-Condensable Gases
PR	Peng-Robinson EoS
P_{reinj}	Reinjection pressure [bar]
$\dot{Q}_{HE, GEO}$	Heat rate of the MHE [kW]
RW	Reinjection Well
SRK	Soave-Redlich-Kwong EoS
TP	Tank-Pipe
TT	Tank-Tank
W_t	Work of the Turbine, [kW]
W_p	Work of the Pump, [kW]
W_{c1}	Work of the Compressor no 1 [kW]
W_{c2}	Work of the Compressor no 2 [kW]
W_{c3}	Work of the Compressor no 3 [kW]
$W_{c, total}$	Work of the Compressor train [kW]
$\dot{W}_{net}$	Net power output [kW]
η_I	Energy efficiency
η_{II}	Exergy efficiency
η_C	Compressor efficiency

Annex 1

The solubility of CO_2 in the geothermal fluid was evaluated applying of a model derived from Duan and Sun [29]. The model is

based on the theory of particle interactions for the liquid phase and on a proper equation of state for the vapour phase. The CO_2 solubility was obtained through the balance of the chemical potential of CO_2 in liquid and vapour phase ($\mu^l_{CO_2}$ and $\mu^v_{CO_2}$ respectively). The chemical potential can be expressed as a function of fugacity for the vapour phase (Equation A.1) and activity for the liquid phase (Equation A.):

$$\mu^v_{CO_2}(T,p,y) = \mu^{v(0)}_{CO_2}(T) + RT\ln f_{CO_2}(T,p,y) = \mu^{v(0)}_{CO_2}(T) + RT\ln(y_{CO2}p) + RT\ln\phi_{CO2}(T,p,y)$$

(A.1)

$$\mu^l_{CO_2}(T,p,m) = \mu^{l(0)}_{CO_2}(T,p) + RT\ln a_{CO2}(T,p,m) = \mu^{l(0)}_{CO_2}(T,P) + RT\ln m_{CO2} + RT\ln\gamma_{CO2}(T,p,m)$$

(A.2)

The fugacity coefficient, ϕ, shows the deviation of a real gas from the ideal behaviour and the activity coefficient, γ, is the ratio of the actual fugacity of a solution to that at the standard state. At equilibrium, $\mu^l_{CO2} = \mu^v_{CO2}$. Therefore, the CO_2 molality m_{CO2}, can be calculated by the following relationship:

$$\ln\frac{y_{CO2}P}{m_{CO2}} = \frac{\mu^{l(0)}_{CO_2}(T,p) - \mu^{v(0)}_{CO_2}(T)}{RT} - \ln\phi_{CO2}(T,p,y) + \ln\gamma_{CO2}(T,p,m)$$

(A.3)

In Equation A.3, $\mu^{v(0)}_{CO2}$ can be set to zero, as the result of the current investigation is affected only by the difference between $\mu^{v(0)}_{CO2}$ e $\mu^{l(0)}_{CO2}$. Therefore, y_{CO2} is determined by:

$$y_{CO2} = \frac{P - P_{H_2O}}{P}$$

(A.4)

p is the total pressure of the mixture ($p_{H2O} + p_{CO2}$). p_{H2O} is the saturation pressure of pure water at the mixture temperature, which is evaluated in the present model using the thermodynamic libraries or by an empiric correlation as in Ref. [29].

The coefficient of activity γ is calculated by the following relationship:

$$\ln\gamma_{CO2} = \sum_c 2\lambda_{CO_{2-c}}m_C + \sum_a 2\lambda_{CO_{2-a}}m_a + \sum_c\sum_a \zeta_{CO_{2-a-c}}m_C m_a$$

(A.5)

where λ and ζ are second order and third order interaction parameters, respectively; m_c and m_a are the molality of cations and anions, respectively. λ, ζ and $\mu^{l(0)}_{CO2}$ are determined by equation (A.6), which is a function of total pressure and temperature only:

$$f(\mathrm{T},\mathrm{p}) = c_1 + c_2T + \frac{c_3}{T} + c_4T^2 + \frac{c_5}{630-T} + c_6p + c_7p\ln T + c_8\frac{P}{T} + c_9\frac{P}{(630-T)} + c_{10}\frac{P^2}{(630-T)^2} + c_{11}T\ln p$$

(A.6)

The c_i coefficients, which are different for λ, ζ and $\mu^{l(0)}_{CO2}$, were obtained from Ref. [29], while the fugacity of the vapour phase was directly computed by the internal libraries available in EES [24].

References

[1] Ármannsson H. CO2 emission from geothermal plants, international geothermal conference. Reykjavík 2003:56−62. S12 Paper103.

[2] Bravi M, Basosi R. Environmental impact of electricity from selected geothermal power plants in Italy. J Clean Prod 2014;66:301−8.

[3] Saner D, Juraske R, Kubert M, Blum P, Hellweg S, Bayer P. Is it only CO2 that matters? A life cycle perspective on shallow geothermal systems,. Renew Sustain Energy Rev 2010;14:1798−813.

[4] CARBFIX project web site. https://www.carbfix.com/. [Accessed 9 March 2019].

[5] Zeyghami M. Performance analysis and binary working fluid selection of combined flash-binary geothermal cycle. Energy 2015;88:76−774.

[6] Walraven D, Laene B, D'haeseleer W. Economic system optimization of air-cooled organic Rankine cycles powered by low-temperature heat sources. Energy 2015;80:104−13.

[7] Erdeweghe SV, Van Bael J, Laenen B, D'haeseleer W. Optimal configuration for a low-temperature geothermal CHP plant based on thermoeconomic optimization. Energy 2019;179:323−35.

[8] Liu Q, Duan Y, Yang Z. Performance analyses of geothermal organic Rankine cycles with selected hydrocarbon working fluids. Energy 2013;63:123−32.

[9] Fiaschi D, Manfrida G, Rogai E, Talluri L. Exergoeconomic analysis and comparison between ORC and Kalina cycles to exploit low and medium-high temperature heat from two different geothermal sites. Energy Conversion and Management 2017;154:503−16.

[10] Liu Q, Duan Y, Yang Z. Effect of condensation temperature glide on the performance of organic Rankine cycles with zeotropic mixture working fluids. Appl Energy 2014;115:394−404.

[11] Fiaschi, D., Colucci, V., Manfrida, G., & Talluri, L. Geothermal power plant case study for a new ORC plant including CO2 reinjection.

[12] Moya D, Aldás C, Kaparaju P. Geothermal energy: power plant technology and direct heat applications. Renew Sustain Energy Rev 2018;94:889−901.

[13] Sohel MI, Sellier M, Krumdieck S. An adaptive design approach for geothermal plant with changing resource characteristics. 2011.

[14] Lei H, Zhu J. Numerical modeling of exploitation and reinjection of the Guantao geothermal reservoir in Tanggu District, Tianjin, China. Geothermics 2013;48:60−8.

[15] Callos V, Kaya E, Zarrouk SJ, Mannington W, Burnell J. Injection of CO2 into liquid dominated two-phase geothermal reservoirs. Proceedings 37th New Zealand Geothermal Workshop 2015;18:20.

[16] O'Sullivan MJ, Yeh A, Mannington WI. A history of numerical modelling of the Wairakei geothermal field. Geothermics 2009;38(1):155−68.

[17] Kaya E, Zarrouk SJ. Simulation of reinjection of non-condensable gas-water mixture into geothermal reservoirs. In: Proceedings of 42nd workshop on geothermal reservoir engineering, stanford university, stanford, California, february 13-15; 2017.

[18] Shafaei MJ, Abedi J, Hassanzadeh H, Chen Z. Reverse gas-lift technology for CO2 storage into deep saline aquifers. Energy 2012;45(1):840−9.

[19] Manente G, Lazzaretto A, Bardi A, Paci M. Geothermal power plant layouts with water absorption and reinjection of H2S and CO2 in fields with a high content of non-condensable gases. Geothermics 2019;78:70−84.

[20] Niknam PH, Habibian M. Experimental study and parallel neural network modeling of hydrocyclones for efficiency prediction. Chem Eng Commun 2015;202(12):1586−90.

[21] Niknam PH, Mortaheb HR, Mokhtarani B. Effects of fluid type and pressure order on performance of convergent−divergent nozzles: an efficiency model for supersonic separation. Asia Pac J Chem Eng 2018;13(2):e2181.

[22] Vaccaro M, Batini F, Stolzuoli M, Bianchi S, Pizzoli R, Lisi S. Geothermal ORC plant case study in Italy: Castelnuovo Val di Cecina pilot project -design and technical features. Proceedings of the European Geothermal Congress 2016: 1−7.

[23] Di Pippo R. Geothermal power plants. Butterworths; 2007.

[24] Nellis FA, Klein FG. Mastering EES. http://fchart.com/ees/mastering-ees.php.

[25] Honeywell International Inc. UniSim® design, operations guide, R460 release. Switzerland. 2017.

[26] Honeywell International Inc. UniSim® design dynamic modeling, reference guide, R460 release. Switzerland. 2017.

[27] Bellani S, Brogi A, Lazzarotto A, Liotta D, Ranalli G. Heat flow, deep temperatures and extensional structures in the Larderello geothermal field (Italy): constraints on geothermal fluid flow. J Volcanol Geoth Res 2004;132:15−29.

[28] Ministero dello sviluppo economico. Risorse geotermiche, available at. https://unmig.mise.gov.it/index.php/it/dati/risorse-geotermiche. [Accessed 15 October 2019].

[29] Duan Z, Sun R. An improved model calculating CO2 solubility in pure water and aqueous NaCl solutions from 273 to 533 K and from 0 to 2000 bar. Chem Geol 2003;193:257−71.

[30] Shariatipour SM, Mackay EJ, Pickup GE. An engineering solution for CO2 injection in saline aquifers. International Journal of Greenhouse Gas Control 2016;53:98−105.

[31] Beggs DH, Brill JP. A study of two-phase flow in inclined pipes. J Petrol Technol 1973;25(5):607−17.

[32] H Niknam P, Talluri L, Fiaschi D, Manfrida G. Improved solubility model for pure gas and binary mixture of CO2-H2S in water: a geothermal case study with total reinjection. Energies 2020;13(11):2883.

[33] Niknam PH, Talluri L, Fiaschi D, Manfrida G. Gas purification process in a geothermal power plant with total reinjection designed for the Larderello area. Geothermics 2020;88:101882.

[34] Parkhurst DL, Appelo CAJ. Description of input and examples for PHREEQC

version 3: a computer program for speciation, batch-reaction, one-dimensional transport, and inverse geochemical calculations (No. 6−A43). US Geological Survey; 2013.

[35] Van Krevelen DW, Hoftijzer PJ, Huntjens FJ. Composition and vapour pressures of aqueous solutions of ammmonia, carbon dioxide and hydrogen sulphide. Recl Trav Chim Pays-Bas 1949;68(2):191−216.

[36] Antoine MC. Nouvelle Relation Entre les Tensions et les Temperatures. C. r. held Seanc. Acad. Sci. Paris 1888;107:681−4.

[37] Niknam PH, Fiaschi D, Mortaheb HR, Mokhtarani B. An improved formulation for speed of sound in two-phase systems and development of 1D model for supersonic nozzle. Fluid Phase Equil 2017;446:18−27.